Estimations of CIN and LFC Associated with Tornadic and Nontornadic Supercells

JONATHAN M. DAVIES

Wichita, Kansas

(Manuscript received 16 September 2003, in final form 10 February 2004)

ABSTRACT

It is generally understood that tornadoes are less likely in environments where surface-based instability is absent and the only convective available potential energy (CAPE) is from elevated parcels originating well above the surface. However, little research has been done to examine tornado occurrence in environments where surface-based CAPE is clearly present, but located above a deep layer of surface-based convective inhibition (CIN) associated with a relatively high level of free convection (LFC) heights. A database of 518 model analysis soundings was collected during 2001–03 from recent versions of the rapid update cycle (RUC) analysis and forecast system. All model sounding profiles were in proximity to selected supercell storms associated primarily with tornado warnings, and were ''nonelevated'' with surface-based CAPE present. This database is used to examine CIN and LFC to determine environments where instability from mixed-layer and surface-based parcels was associated with significant negative buoyancy in low levels. Findings evaluated for tornadic and nontornadic supercells show that the frequency of F1–F4 intensity tornadoes decreased significantly for increasing CIN and LFC height. The fact that tornado warnings were issued for many nontornadic supercells with large CIN and high LFC heights in the database examined suggests that better awareness of environments having increased CIN and LFC characteristics may be useful operationally in discriminating between some tornadic and nontornadic supercell settings.

1. Introduction

Tornadoes are considered less likely to occur with ''elevated'' supercells found in storm environments where the only instability is from parcels that originate well above the surface (e.g., Rasmussen and Blanchard 1998, hereafter RB98). Elevated convection as defined by Colman (1990, hereafter C90) has no surface-based convective available potential energy (CAPE, Moncrief and Miller 1976). But, many thunderstorm environments have significant surface-based CAPE present *above* a deep layer of convective inhibition (CIN, Colby 1984), signified by a large area of negative buoyancy below the positive CAPE area on a thermodynamic diagram. Therefore, a distinction can be made between thunderstorm settings that have *no* surface-based CAPE, with positive CAPE associated only with lifted parcels from well above the surface (*elevated* storm environments as defined by C90, Fig. 1a), and thunderstorm settings that involve positive surface-based CAPE located above a large layer of surface-based CIN (Fig. 1b) associated with a relatively high level of free convection (LFC). Severe storms and supercells occur in a variety of thermodynamic settings, including profiles and configurations similar to Fig. 1b. It is possible that such variations may have an effect on tornado potential.

This empirical examination uses estimations of CIN and LFC to identify environments with CAPE that may be located above large CIN, as in Fig. 1b. A large database of analysis profiles from recent versions of the rapid update cycle (RUC) analysis and forecast system (Benjamin et al. 2004), similar to Thompson et al. (2003, hereafter T03), is used to approximate environments of tornadic and nontornadic storms, covering a wide range of CIN and LFC values. The objective is to better describe and assess CIN and LFC environments relative to supercell tornado occurrence in a variety of estimated storm settings.

Section 2 will discuss the possible relationship of CIN and LFC to tornado potential based on prior studies. Methodology of database selection and parameter computation is presented in sections 3 and 4. Section 5 focuses on the virtual temperature correction, which deserves brief discussion because of its effect on the computation of CIN and LFC. Section 6 presents database results regarding tornadic and nontornadic cases. Environments with both large CIN and large vertical shear are discussed in section 7. Case examples presented in section 8 include both cool and warm sector environments having relatively large CIN and high LFC heights. Section 9 briefly contrasts LFC with lifting condensation level (LCL) in environments with large CIN. The final section is a summarizing discussion with conclusions.

Corresponding author address: Jonathan M. Davies, 3206 N. Westwind Bay, Wichita, KS 67205-2528.
E-mail: jdavies1@cox.net

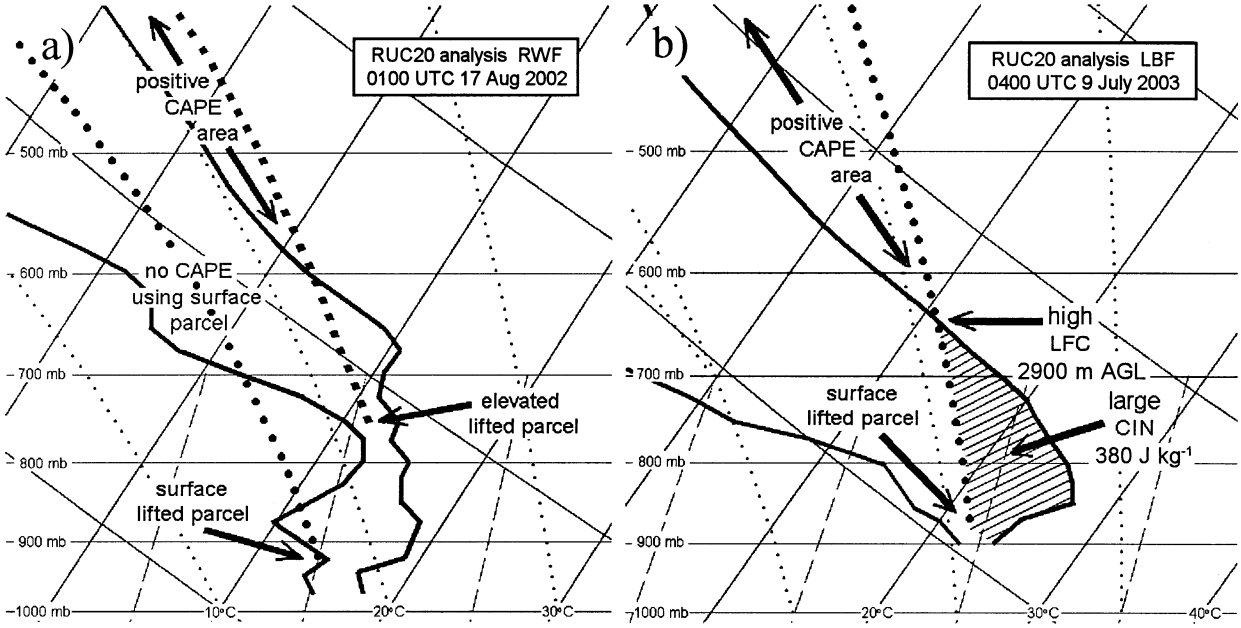

FIG. 1. Lower portion of skew *T*–log*p* diagrams illustrating (a) *elevated* environment (no surface-based CAPE), and (b) environment with positive surface-based CAPE above large CIN, using RUC-20 analysis profiles associated with documented supercells. Thermodynamic profiles of dewpoint and temperature are shown as thick solid lines/curves. Important features are labeled with arrows. Curves with thick round dots show surface parcel ascents. Curve with thick square dots in (a) is elevated lifted parcel ascent. Hatching in (b) denotes negative area of surface-based CIN. For viewing simplicity, the virtual temperature correction is not included.

2. Possible relevance of CIN and LFC to tornado potential

Supercell thunderstorms can occur in environments where air parcels originating near the ground realize their instability only after forced ascent through a deep layer of negative buoyancy, as shown in Fig. 1b. These environments will, by definition, be characterized by sizable CIN and a relatively high LFC. How storms develop in large CIN environments is not clear, but storm initiation in many such settings may be facilitated by parcels having smaller CIN that originate a significant distance above the ground, similar to elevated environments as defined in C90.

RB98 found in their database that soundings associated with supercells producing significant tornadoes tended to have less CIN than soundings associated with nontornadic supercells. Although RB98 were unable to assess which environments in their database were elevated as in C90, because they used the lowest 1000-m mixed-layer lifted parcels rather than surface parcels, their results do suggest that CIN (and by association, LFC height) may have some degree of impact on tornado potential. Updrafts in environments with CAPE located above an area of large CIN require significant vertical pressure gradient forces (e.g., Rotunno and Klemp 1982) to lift near-surface parcels past the LFC. Even with a sizable amount of CAPE above the large CIN, the stretching of parcels by the updraft may be reduced or inhibited at the surface due to the strong area of negative buoyancy in low levels. Because tornadoes are understood to be a surface phenomenon (e.g., Markowski et al. 2002), it is possible that this kind of thermodynamic setting may interfere with tornado development.

This study is an opportunity to see if the empirical results from RB98 regarding CIN hold forth using both mixed-layer and surface-based estimates of CIN and LFC from model-derived soundings. If so, it may be possible to better define what comprises truly ''large'' CIN or ''high'' LFC heights that could negatively affect tornado potential.

Results from RB98 and others (e.g., Craven et al. 2002a) have shown supercell tornadoes to be associated with lower LCL heights. However, in environments where CIN is relatively large, LCL (an estimate of cloud base) may be a poor diagnostic tool because it gives no information about the specific level where positive CAPE begins (the LFC) as parcels continue to ascend above cloud base. LCL and LFC will be examined together in a later section with regard to environments having relatively large CIN.

3. Database methodology

The database used in this study was made up of 518 model analysis profiles associated with supercells having positive surface-based CAPE. This definition excluded elevated storms as in C90 (see Fig. 1a), but included environments with positive surface-based CAPE located above large CIN (see Fig. 1b). Exclusion of

TABLE 1. Description and summary of profiles in the D03 database used for this study.

Tot profiles	RUC-2 (2001–02)	RUC-20 (2002–03)
518	199	319

All profiles associated with radar-indicated supercells that had tornado warnings (477 cases) or severe thunderstorm warnings (41 cases), 2001 through mid-2003.

All profiles located within 100 km and 90 min prior to or during warned period of associated supercell, within inflow air mass east-northeast through south-southwest of warned storm.

	Associated tornado reports						
Nontornadic	F0	F1	F2	F3	F4	F5	Tot
243	108	62	62	27	16	0	518

environments having no surface-based CAPE eliminated the problem of being unable to distinguish between elevated and nonelevated storms in the database of RB98.

Profiles were collected from January 2001 through July 2003 using RUC analysis soundings east of the Rocky Mountains, similar to those in T03 with vertical resolution of 25 hPa at standard isobaric levels above the surface. T03 concluded that RUC-2 analysis profiles of this type were a reasonable proxy for estimating near-storm environments in most cases. Of the profiles collected for this study, 199 were from the old RUC-2 model (40-km resolution, Benjamin et al. 1998), and 319 were from the RUC-20 model that became operational in 2002 (20-km resolution, Benjamin et al. 2002). Because T03 suggested from operational experience at the Storm Prediction Center (SPC) that soundings from the two model versions were compatible, profiles from both sources were treated the same for purposes of this study. The resulting collection of profiles will be referred to as simply the ''D03 database.''

Table 1 gives an overview of the D03 database profiles and associated storm cases. Selection was based primarily on supercells that were *tornado warned* by National Weather Service (NWS) offices, an approach that was notably different than in T03. Radar indication of storm rotation according to a *specific warning text* was a key criteria used in selecting 477 cases for the database. Low-resolution lowest-level base reflectivity radar data were saved with other cases considered for inclusion in the database, resulting in selection of an additional 41 cases that were associated with severe thunderstorm warnings. In these additional cases, reflectivity characteristics consistent with supercells (e.g., hook echoes or inflow notches, Lemon 1977) were evident for 30 min or more. The National Oceanic and Atmospheric Administration (NOAA) publication *Storm Data* and additional information from NWS offices were used to verify tornadoes and assign ratings. Because of reliance on tornado warnings and radar reflectivity data apart from explicit velocity features (significant velocity characteristics were implied by the text of tornado warnings), the overall data selection methodology was not as rigorous as T03 in defining supercells from a radar perspective. However, it had the advantage of being tied to operational reality by emphasizing supercells with radar characteristics impressive enough to prompt tornado warnings in real time by NWS meteorologists.

Other selection criteria were similar to T03, but not as tightly defined regarding time and location proximity. All profiles were within 90 min prior to, or during, an associated storm's warned period (the majority of profiles were within 60 min) and located within 100 km to the east-northeast through south-southwest of the associated storm to approximate general inflow environments. Though less restrictive in selection methodology than the database in T03, the D03 database, by virtue of its large size, provides a useful collection of model analysis profiles associated with a broad range of supercell thunderstorms. The profiles were collected and analyzed only as *estimations* of nearby storm inflow environments.

4. Computation methodology

Because temperature errors for RUC profiles in T03 were found to be largest near the ground, actual surface observations were used to update the profiles in this study for better estimation of the environment and associated parameters. The SPC uses observed surface data in a similar fashion to modify short-term forecast RUC profiles for generating operational mesoanalysis fields (Bothwell et al. 2002). For this study, representative surface observations were collected at the same site (or nearby sites in the same air mass when same-site data were unavailable) for the same valid time as each of the profiles in the D03 database. These were then compared to the model analysis surface data. If the model analysis differed more than 0.5°C from the observed surface temperature or dewpoint, the observed value was blended into the profile using linear interpolation in low levels, depending on the shape of the profile. If a significant inversion was present within the lowest 150 hPa, the interpolation and modification was limited to the part of the profile *below* the inversion. Otherwise, the interpolation and modification was applied through 150 hPa above ground level. T03 did not incorporate observed surface data for their parameter computations, a notable difference between the two databases.

Thermodynamic computations using mixed-layer lifted parcels in the lowest 100 hPa were emphasized because that method appears to be a more realistic, operational approach based on observed cloud bases as in Craven et al. (2002b), and was used by T03. Surface-based lifted-parcel computations were also examined to look at thermodynamic characteristics that may relate to tornadoes as a surface-based phenomenon (e.g., Markowski et al. 2002). Hereafter, ''ML'' is used to denote thermodynamic parameters computed using mixed-layer

TABLE 2. Mean difference in value and percent change in MLCAPE, MLCIN, and MLLFC in the D03 database *with* (COR) and *without* (UNCOR) the virtual temperature correction.

	MLCAPE	MLCIN	MLLFC
Mean diff (COR−UNCOR)	+145 J kg^{-1}	−21 J kg^{-1}	−247 m
Mean % change (COR/UNCOR)	+7.8%	−26.7%	−12.2%

parcels (e.g., MLCAPE, MLCIN, MLLFC, etc.); ''SB'' is used to denote surface-based computations (e.g., SBCIN, SBLFC, etc.). All LFC heights are given above ground level (AGL).

Occasionally, superadiabatic low-level lapse rates resulted from combining observed surface data with model analysis soundings having temperatures notably cooler than observed in the lowest part of profiles, even with the profile modification methodology described earlier. This sometimes resulted in an LFC height that was computed to be lower than the LCL, a false situation generated by a poor low-level RUC analysis. For consistency when such cases were encountered in this study, the LFC was set to be equal to the LCL—a more physically realistic assumption. Also, when multiple LFC heights were encountered with some profiles due to certain inversion shapes, the lowest LFC was used. An exception was when total CIN was relatively large (>50 J kg^{-1}, more than double the amount RB98 found associated with most significant supercell tornadoes in their database); in those cases the total CIN in the profile was considered significant and the highest LFC was deemed more relevant.

As in RB98 and T03, the virtual temperature correction (Doswell and Rasmussen 1994) was applied to computations and is discussed briefly in the next section because of the effect it can have on magnitude of CIN and LFC values.

5. Impact of the virtual temperature correction on CIN and LFC computations

From Doswell and Rasmussen (1994), the virtual temperature correction (VTC) incorporates virtual temperature to properly calculate density when computing CAPE and related thermodynamic parameters. This is an important issue because CAPE accounts for the difference in density between a rising parcel and its environment. Typically, this correction will increase CAPE, reduce CIN, and lower LFC height (the VTC has no effect on LCL). Because the VTC has most of its impact in low levels, and on profiles that have a deep moist layer (adding water vapor to a parcel makes it less dense), its effect on parameters such as CIN and LFC in thunderstorm situations deserves discussion.

To examine the impact of the VTC, all profiles in the D03 database were used to compute MLCAPE, MLCIN, and MLLFC *with* and *without* the VTC. Comparison between the two methods is shown in Table 2, giving the mean differences and percentage changes between *corrected* values (with the VTC) and *uncorrected* values (without the VTC). It can be seen that the VTC on average had a larger relative impact on CIN and LFC than on total CAPE. The VTC reduced uncorrected MLCIN in one-third of the profiles by 25 J kg^{-1} or more (not shown), and 13% of the profiles were reduced by 50 J kg^{-1} or more. In a few large CIN cases involving significant low-level density differences (e.g., a very moist layer located below a strong temperature inversion), corrected MLCIN differed from uncorrected MLCIN by more than 75 J kg^{-1}, and corrected MLLFC differed from uncorrected MLLFC by more than 800 m.

These results suggest that the impact of the VTC is not always negligible regarding CIN and LFC. The VTC was recommended by Doswell and Rasmussen (1994) to be a standard way of computing CAPE and comparing soundings, but operational software applications used by forecasters at the time of this paper differ as to whether the VTC is included in thermodynamic computations. Because of this, some initial results presented in section 6 will be shown using *both* methods for appropriate comparison.

6. Results

Figures 2 and 3 show the distribution of MLCIN (similar to RB98) and MLLFC in the D03 database for nontornadic cases, weak tornadic cases (F0–F1), and significant tornadic cases (F2–F4) using box and whisker plots. Results using the VTC are shown in Figs. 2a and 3a for comparison with results not using the VTC in Figs. 2b and 3b. Whiskers extend to the 10th and 90th percentiles for consistency with RB98 and T03.

The tornadic cases in Figs. 2 and 3 had a tendency to be associated with smaller MLCIN and lower MLLFC heights, with the largest differences in distribution occurring between nontornadic and significant tornadic supercells, similar to MLCIN results in RB98. The 90th percentiles for the nontornadic cases extended noticably higher (MLCIN near or above 200 J kg^{-1}, MLLFC above 3000 m) than for the significant tornado cases (MLCIN 60–100 J kg^{-1}, MLLFC 2000–2500 m), suggesting that MLCIN was noticably ''large'' and LFC heights noticably high for a number of cases in the upper half of the nontornadic distributions.

The impact of the VTC is seen by comparing Figs. 2a and 3a to Figs. 2b and 3b, with the median values and upper halves of the distributions most affected. Because the VTC in the larger CIN cases typically reduced MLCIN by 25–50 J kg^{-1} and MLLFC by 200–400 m, forecasters should be aware of potential computation differences in operational software applications, de-

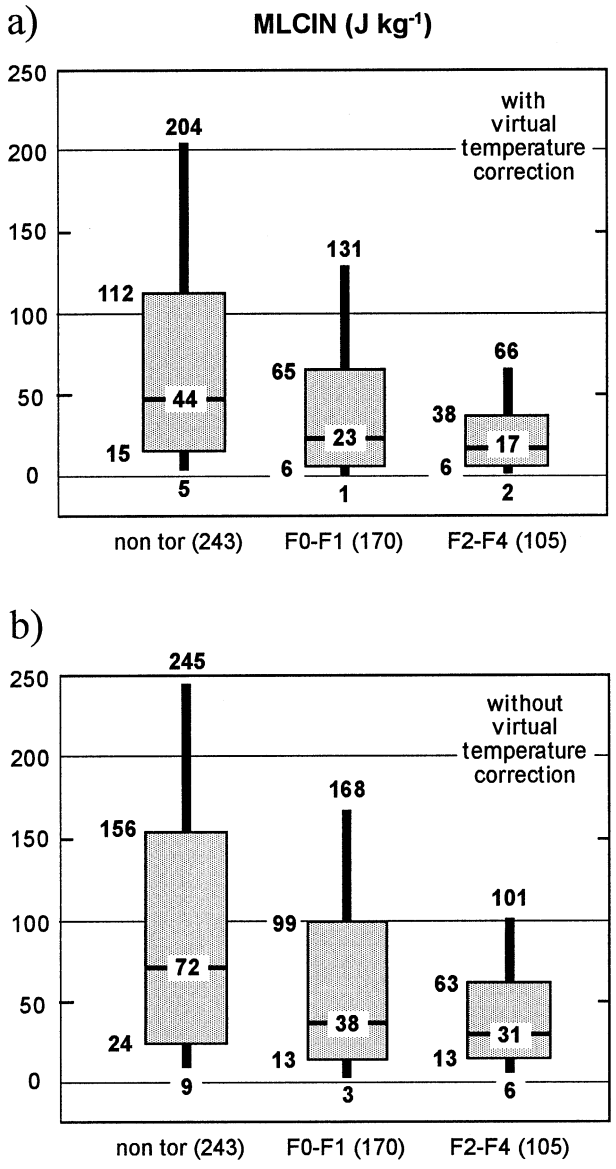

FIG. 2. Box and whisker plots of MLCIN (J kg^{-1}) for profiles in the D03 database computed (a) with and (b) without the virtual temperature correction. Data are grouped as cases with (left) no tornadoes (''non tor''), (middle) weak tornadoes (''F0–F1''), and (right) significant tornadoes (''F2–F4''). Numbers in parentheses give total cases in each category. Boxes denote 25th–75th percentiles, with horizontal bar showing median value. Whiskers extend to the 10th and 90th percentiles.

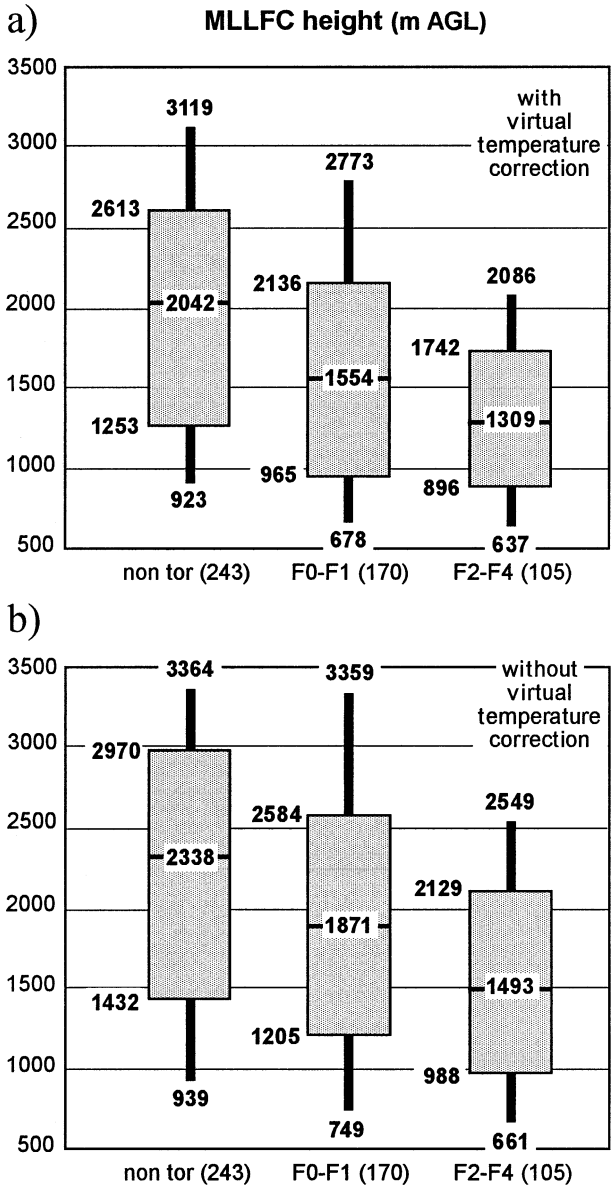

FIG. 3. As in Fig. 2, except MLLFC height (m AGL) for profiles in the D03 database.

pending on whether the VTC is included. For simplicity, hereafter only results incorporating the VTC will be shown and discussed.

While the box and whisker plots in Figs. 2 and 3 were useful in showing the broad distribution of cases within each category, a more detailed look at the tornadic cases was desired for qualitatively estimating CIN amounts and LFC heights most related to tornado occurrence. Figures 4 and 5 show the number of tornadoes by MLCIN and MLLFC from the D03 database using ascending 25 J kg^{-1} and 500-m range categories, respectively. Because F1 tornadoes do cause fatalities and are a serious concern to forecasters (five F1 cases in the D03 database were associated with deaths), F1 tornadoes were grouped with significant (F2–F4) tornadoes in Figs. 4 and 5, while F0 tornadoes were excluded.

The drop in the number of tornadoes in Fig. 4 when MLCIN was larger than 50 J kg^{-1} suggests that MLCIN somewhere between 50 and 100 J kg^{-1} is where low-level negative buoyancy may become large enough to possibly have an impact on the likelihood of tornadoes. The same is suggested by MLLFC heights somewhere between 2000 and 3000 m (Fig. 5). Furthermore, only one tornado (F2 intensity) occurred with MLCIN >

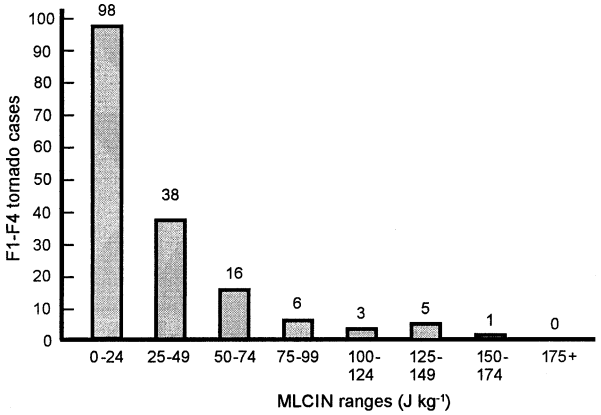

FIG. 4. Number of F1–F4 intensity tornadoes from the D03 database by MLCIN (using the virtual temperature correction) in ascending ranges of 25 J kg^{-1}.

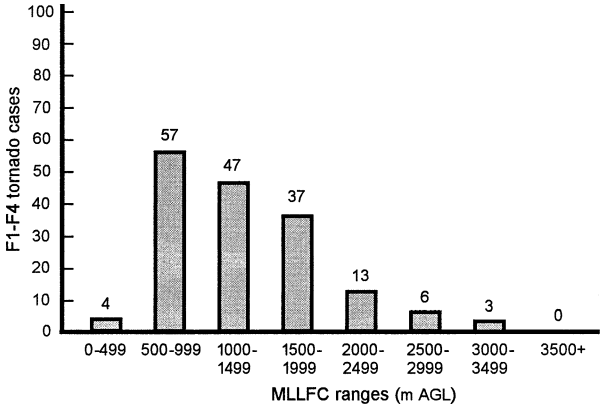

FIG. 5. As in Fig. 4, except MLLFC in ascending ranges of 500 m AGL.

150 J kg^{-1} and only three tornadoes (one of F1 intensity, two of F2 intensity) occurred with MLLFC $>$ 3000 m. MLCIN and MLLFC near and above these values may help define low-level thermodynamic environments where negative buoyancy is large to a degree that the likelihood of significant tornadoes is considerably reduced.

Because thermodynamic parameters computed from surface-based parcels appear to relate to tornado likelihood (Markowski et al. 2002), tornado cases were examined relative to CIN and LFC using surface-based computations, which was not done in RB98. The number of F1–F4 tornadoes categorized by increasing SBCIN and SBLFC (not shown) was very similar to Figs. 4 and 5, with a nearly identical drop in tornadoes when SBCIN was 50–100 J kg^{-1} or larger and SBLFC was 2000–3000 m or higher. As in Fig. 4, only one tornado of F1–F4 intensity occurred with SBCIN larger than 150 J kg^{-1}. This similarity in the distribution of tornadoes suggests that surface-based and mixed-layer parcels shared somewhat similar CIN and LFC characteristics in most tornado cases in the D03 database.

Table 3 shows the number of cases in the D03 database where SBCIN was less than MLCIN or at least roughly equal to it (within 10 J kg^{-1} to allow for small errors in model-derived profiles and estimated parameters) when comparing nontornadic–F0 cases and F1–F4 tornado cases. This table indicates that surface parcels in a larger percentage of F1–F4 tornado cases (75%) than in nontornadic or F0 cases (55%) had very close to the smallest amount of energy (if not the least amount) required to reach the LFC, suggesting that convection in the majority of tornado cases in the D03 database was strongly surface based. Although mixed-layer lifted parcels in general appear to be more realistic in representing low-level mixing processes when computing thermodynamic parameters (Craven et al. 2002b), Table 3 suggests that it could be important to compare both mixed-layer and surface-based parcel computations of CIN and other thermodynamic parameters in potential tornado situations. If surface-based parcels compared to mixed-layer parcels, have less CIN and require less lifting energy in settings with positive CAPE and significant vertical shear, this could suggest increased tornado potential. Similarly, SBCIN noticably larger than MLCIN could suggest a possible decrease in the likelihood of tornadoes, although this idea certainly requires further investigation.

7. Environments with large CIN and large vertical shear

Large CIN acts as a layer of stability to parcels attempting to ascend from below. As suggested in section 2, this situation may inhibit or reduce parcel ascent and stretching near the ground, and may be one reason that tornado frequency with supercells tends to drop off as CIN becomes larger and LFC heights higher. However, in cases with strong vertical shear interacting with an updraft, resulting shear-induced vertical pressure gradients could induce significant upward accelerations to help overcome this. That may suggest why some supercells can produce tornadoes in environments where CIN appears relatively large (e.g., 50–150 J kg^{-1}, see Fig. 4).

To examine this, Fig. 6 shows mean values of the energy–helicity index (EHI; Hart and Korotky 1991; Davies 1993) for ascending MLCIN in categories of 50 J kg^{-1}. This revised EHI formulation (Rasmussen 2003), combining total MLCAPE and 0–1-km storm-

TABLE 3. Comparison showing number and percentage of cases where SBCIN was less than MLCIN or roughly equal to MLCIN (within 10 J kg^{-1}) for nontornadic or F0 intensity tornado cases, F1–F4 intensity tornadic cases, and all cases from the D03 database.

Nontornadic and F0	F1–F4	All cases
192 of 351 (55%)	125 of 167 (75%)	317 of 518 (61%)

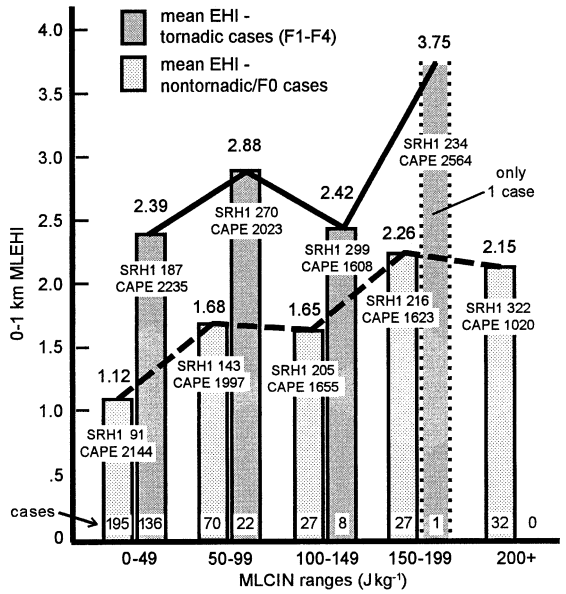

FIG. 6. Mean 0–1-km MLEHI values for nontornadic–F0 intensity tornado cases (lightly shaded bars) compared to F1–F4 intensity tornadic cases (heavily shaded bars) from the D03 database by MLCIN in ascending ranges of 50 J kg^{-1}, computed using the virtual temperature correction. Solid line shows trend of mean MLEHI for tornadic F1–F4 cases, and dashed line shows corresponding trend for nontornadic and F0 cases. Associated mean values of 0–1-km SRH (''SRH1'') and MLCAPE (''CAPE'') are annotated on each bar, with the number of cases shown at the bottom.

relative helicity (SRH, Davies-Jones et al. 1990), has been found to have significant association with tornadic supercell environments (e.g., T03):

$$\text{MLEHI}_{0\text{–}1} = (\text{MLCAPE} \times \text{SRH}_{0\text{–}1})/160\,000. \quad (1)$$

It may be notable that mean 0–1-km MLEHI values in Fig. 6 were consistently *large* (near 2.0 and greater) for F1–F4 tornado cases (''tornadic'') compared to nontornadic–F0 cases (''nontornadic''). This is mainly a result of *increases* in low-level wind shear as measured by 0–1-km SRH (see annotated values in Fig. 6) for tornado cases in the larger MLCIN categories (>50 J kg^{-1}). For both equal and unequal variances in each of the MLCIN categories in Fig. 6, *t* tests show that the tornadic and nontornadic MLEHI comparisons were statistically significant at the 95% confidence level for cases with MLCIN < 100 J kg^{-1} (including cases with MLCIN 50–99 J kg^{-1}). However, the relative number of tornadic to nontornadic cases was too small for statistical significance in the MLEHI comparisons with MLCIN ≥ 100 J kg^{-1}. Therefore, it should be emphasized that little or no discrimination using 0–1-km MLEHI or 0–1-km SRH can be made between tornadic and nontornadic cases for MLCIN categories larger than 100 J kg^{-1} in the D03 database. Nonetheless, Fig. 6 does at least suggest that some supercells are able to generate tornadoes in larger CIN/higher LFC environments when supported by large EHI, resulting from large amounts of low-level SRH. It can also be emphasized that there were no F1–F4 tornado cases when MLCIN was greater than 200 J kg^{-1}.

In addition to low-level wind shear, deeper-layer wind shear interacting with an updraft may also be important in tornado cases involving larger CIN. It is worth noting that shear in the 0–6-km layer (e.g., T03) for tornadic supercells in the larger MLCIN categories from the D03 database was typically large, near 25 m s^{-1} or greater (not shown).

It may also be worth noting that SBCIN was roughly equal to or less than MLCIN (not shown) in eight of the nine tornado cases of F1–F4 intensity in Fig. 6, having MLCIN ≥ 100 J kg^{-1}; in five of these cases SBCIN was less by 20 J kg^{-1} or more. While no conclusions can be made from such a small sample of tornadoes associated with MLCIN ≥ 100 J kg^{-1}, this could hint at the possible importance of comparing surface-based thermodynamic results to mixed-layer results as discussed at the end of section 6.

8. Cool and warm sector environments with large CIN/high LFC

Similar to thunderstorm environments with truly elevated characteristics (no surface-based CAPE) as discussed by Maddox et al. (1980), C90, and Doswell et al. (2002), positive CAPE environments with large CIN from both surface-based and mixed-layer parcels are not uncommon immediately north of thermal boundaries. Large CIN environments can also occur in the warm sector associated with a warm mixed layer aloft and a resulting inversion, rather than an analyzed front or boundary on a surface map associated with cool surface temperatures.

Presented briefly in this section are some examples of settings involving differing CIN and LFC environments. Two cases (one nontornadic and one tornadic) were located in the cool sector north of fronts, and two other cases (one nontornadic and one tornadic) were located in the warm sector. Fields generated using the RUC-based mesoanalysis at SPC (Bothwell et al. 2002) available online in real time (http://www.spc.noaa.gov/exper/mesoanalysis/), and profiles from the Eta Data Assimilation System (EDAS; Rogers et al. 1996) available online in archive form (http://www.arl.noaa.gov/ready/amet.html) from NOAA's Air Resources Laboratory (ARL), are shown as analysis examples from widely used operational models. MLCAPE and 0–1-km SRH are shown separately in the first two cases to illustrate the magnitude of low-level wind shear; in two other cases these fields are combined as 0–1-km MLEHI for figure simplicity. Mixed-layer thermodynamic computations are used as in Craven et al. (2002b), but surface-based computations (e.g., SBCAPE and SBCIN available on the SPC mesoanalysis site) could also be useful for comparison as discussed in sections 6 and 7.

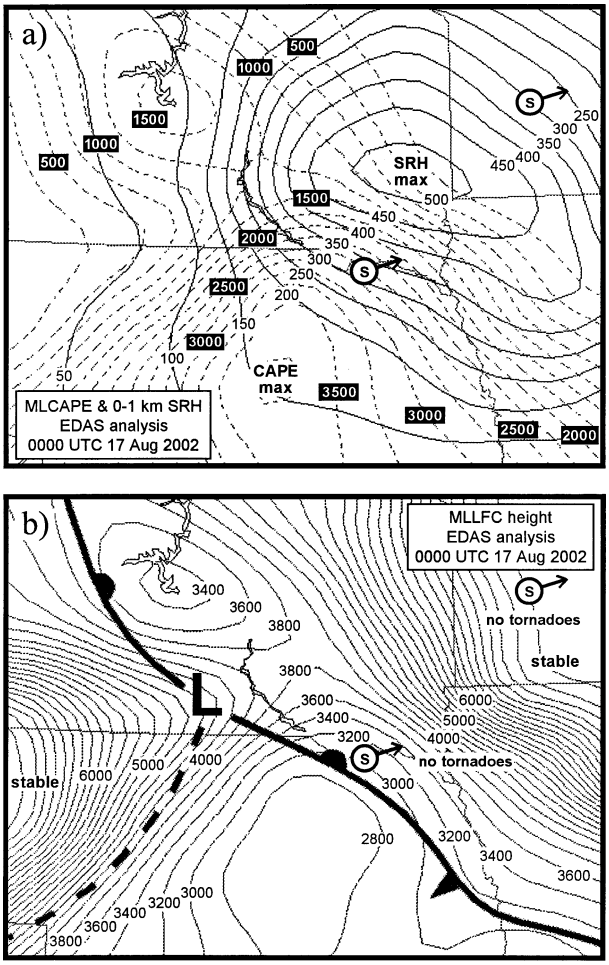

FIG. 7. Parameter fields of (a) MLCAPE (dashed, in 250 J kg^{-1} increments) and 0–1-km SRH (solid, in 50 m^2 s^{-2} increments), and (b) MLLFC height (in 200-m increments AGL) from Eta/EDAS analysis at 0000 UTC 17 Aug 2002 over the Nebraska–South Dakota–southwest Minnesota area. Surface features are shown in (b). Location and general movement of supercells (''S'' within circles) between 0000 and 0200 UTC are also shown in both (a) and (b).

a. Example 1—Stationary cool sector environment (nontornadic)

On 16 August 2002, over northeast Nebraska, southeast South Dakota, and southwest Minnesota, unseasonably strong wind shear at late afternoon was located north of a stationary front reinforced by cool outflow from morning convection. Figure 7 depicts analysis fields computed using data from the EDAS archive; Fig. 7a shows MLCAPE and 0–1-km SRH at 0000 UTC 17 August 2002, and Fig. 7b shows surface features and MLLFC heights at the same time. The locations of two tornado-warned supercells during early evening are also shown in both figures—one just north of the front near the Nebraska–South Dakota border, and another deep in the cool air over southwest Minnesota. Neither storm produced tornadoes.

Although the CAPE–shear combinations were very strong, MLLFC heights (>3000 m, Fig. 7b) suggest that there may have been too much low-level negative buoyancy to support tornadic supercells with cool surface temperatures immediately north of the front. Temperatures across the front contrasted by nearly 10°C (roughly 20°F), and surface maps (not shown) indicated that the cool surface air remained nearly stationary through late afternoon and evening, with little displacement or modification of the air mass north of the front. The warm sector environment to the south also appeared to have relatively high MLLFC heights (2700–3000 m). Further north, the Minnesota supercell was completely elevated, with no surface-based CAPE present in that environment.

In this case, analysis profiles from both the RUC-20 model and the Eta Model (via the EDAS archive) depicted large SBCIN and MLCIN (200 J kg^{-1} or more, not shown) near the stationary front, even though the EDAS profiles were of much lower resolution. It should be noted from Baldwin et al. (2002) that CIN and LFC are affected by the convection scheme in the National Centers for Environmental Prediction (NCEP) Eta Model when shallow convection is forecast, which can result in smaller values than observed. But, recent operational experience also suggests that horizontal patterns and gradients of MLCIN and MLLFC from both the RUC and Eta Models tend to be similar, with RUC-derived values often a little larger.

b. Example 2—Cool sector environment with an advancing warm front (tornadic)

This case on the morning of 24 December 2002 in southeast Alabama and southwest Georgia also involved a cool sector environment, but differed from the prior example in that an advancing warm front was involved.

Figure 8a depicts MLCAPE and 0–1-km SRH at 1200 UTC using data from the EDAS archive, showing strong low-level shear that was located north and east of a warm front over southern Alabama (Fig. 8b). The MLCIN field derived from the same data for the same time in Fig. 8b showed a large CIN environment (>150 J kg^{-1}) north of the front. However, in contrast to the prior example, the warm front was *advancing* with strong low-level warm advection and a change in air mass taking place. For example, the observed surface dewpoint just south of the Alabama border at Marianna, Florida (not shown), increased from 17° to 20°C (63° to 68°F) during the period 1100–1300 UTC. An F1 tornado (track shown in the figures) developed shortly before 1300 UTC, associated with a supercell embedded in a squall line near Dothan, Alabama, causing 10 injuries along its 50-km path into Georgia.

In this tornadic case, the presence of a reduced CIN environment to the southwest (MLCIN < 50 J kg^{-1}, see Fig. 8b) that was advancing as a warm front and slowly displacing the cool air in low levels was probably very significant. This highlights the importance of mon-

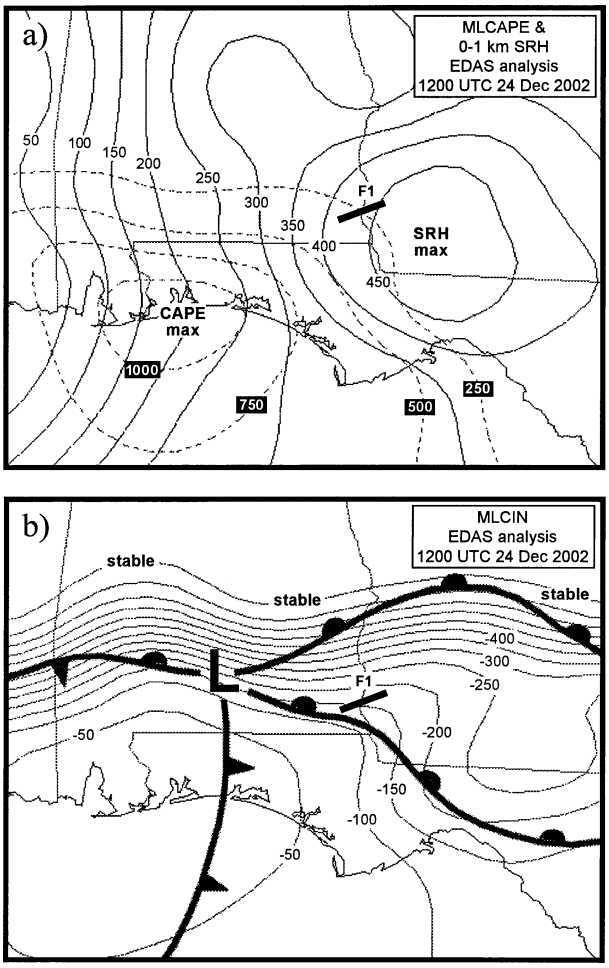

FIG. 8. Parameter fields of (a) MLCAPE and 0–1-km SRH, and (b) MLCIN (in 50 J kg^{-1} increments) from Eta/EDAS analysis similar to Fig. 7, except at 1200 UTC 24 Dec 2002 over the Florida panhandle, southern Alabama, and southern Georgia. Surface features are shown in (b). Track of F1 tornado between 1200 and 1400 UTC is also shown in both (a) and (b).

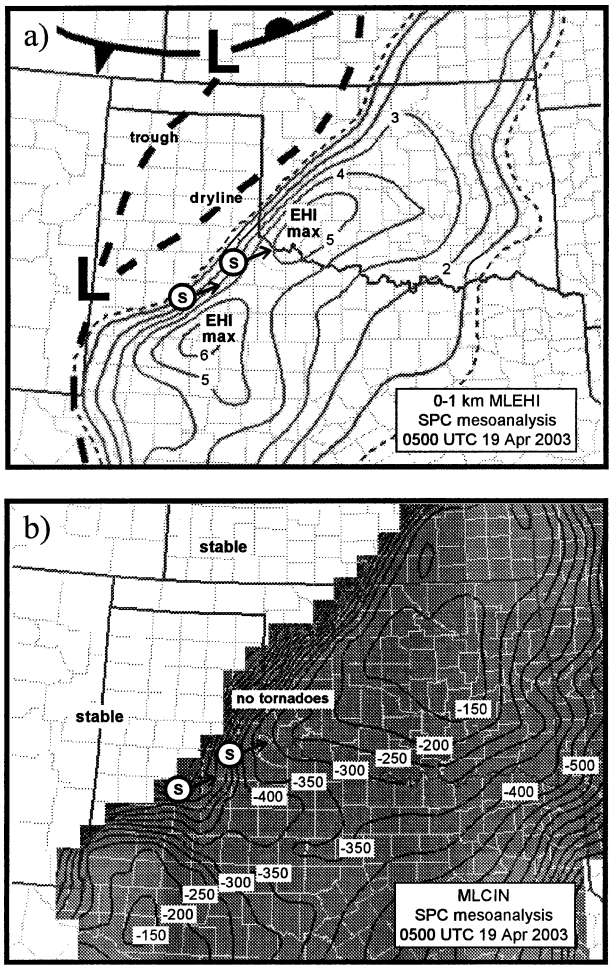

FIG. 9. Parameter fields of (a) 0–1-km MLEHI, and (b) MLCIN (in 50 J kg^{-1} increments) from RUC-based SPC mesoanalysis at 0500 UTC 19 Apr 2003 over the southern plains. Surface features are shown in (a). Area where MLCIN $>$ 100 J kg^{-1} is shaded in (b). Location and general movement of selected supercells (''S'' within circles) between 0500 and 0700 UTC are also shown in both (a) and (b).

itoring evolution of surface observations, map features, and diagnostic fields that may signal rapid changes in near-storm environment, rather than reliance only on periodic model forecasts. Model trends (not shown) on the morning of 24 December 2002 did suggest some northward displacement of the cool surface environment, but the degree of environment evolution near the warm front was most evident from changes in local surface observations.

Also notable is the fact that Eta-based profiles in this case appeared more representative than RUC-based profiles (not shown), regarding the thermodynamic environment near and south of the warm front. Comparing profiles from EDAS and the RUC-20 analysis to the 1200 UTC sounding released at Tallahassee, Florida (not shown), the Eta Model analysis better captured observed near-saturation conditions in the lowest 3 km not seen on nearby RUC-based profiles having a questionable dry layer not far above ground. Precipitation in the area and observed strong low-level warm advection suggested that Eta-based profiles were thermodynamically more realistic near the warm front in this case.

c. Example 3—Nighttime warm sector environment (nontornadic)

During the late night of 18 April 2003, strong supercells moved across northwest Texas and southwest Oklahoma. Figure 9a shows surface features and 0–1-km MLEHI (combining MLCAPE and 0–1-km SRH as in Fig. 6) from the RUC-based SPC mesoanalysis for 0500 UTC 19 April 2003. Figure 9b shows MLCIN from the same data. Although CAPE–shear combinations and resulting EHI values were large over the area where tornado-warned supercells occurred (locations shown in

both figures), CAPE also appeared to be located above a deep layer of large CIN. Eta-based (not shown) and RUC-based profiles both suggested that large MLCIN values (150–400 J kg^{-1}) and high MLLFC heights (near 3000 m or above, not shown) were present in a broad area across most of the warm sector (see shaded area in Fig. 9b). SBCIN and SBLFC (not shown) were similarly impressive in showing large low-level negative buoyancy. No tornadoes occurred with any of the supercells.

Warm sector thunderstorms occur frequently at night in the plains during spring and summer. Like this example, many of these environments have large CIN and high LFC heights due to diurnal low-level cooling below a warm mixed layer aloft. This may be one reason why late night and early morning tornadoes do not occur often in the plains. Supercell tornadoes do occasionally develop in warm sector environments having large CIN if wind shear is very strong (see section 7), particularly if storms occur closer in time to surface heating when enhanced low-level lapse rates can increase CAPE and reduce the depth of the large CIN layer.

d. Example 4—Daytime warm sector environment (tornado outbreak)

An outbreak of tornadoes occurred over eastern Kansas and western Missouri on the afternoon and evening of 4 May 2003. Figure 10a shows surface features and 0–1-km MLEHI at 2100 UTC from the RUC-based SPC mesoanalysis as in the prior example, while Fig. 10b shows approximated MLLFC heights. Several supercells developed from north to south across eastern Kansas, producing tornadoes (tracks shown in both figures) and causing 10 deaths from 2100 to 2330 UTC.

This case is an example of thunderstorm development in response to a strong dynamic system aloft (not shown) over an area of low LFC heights *collocated* with strong CAPE–shear combinations. Eta-based (not shown) and RUC-based profiles both suggested small MLCIN ($<$25 J kg^{-1}, not shown) and very low MLLFC heights (near or below 1000 m) across much of the warm sector. In contrast, the environment north and east of the slow moving warm front near Kansas City transitioned rapidly to large CIN and high LFC characteristics, a possible limiting factor to the northward extent of tornadic storms.

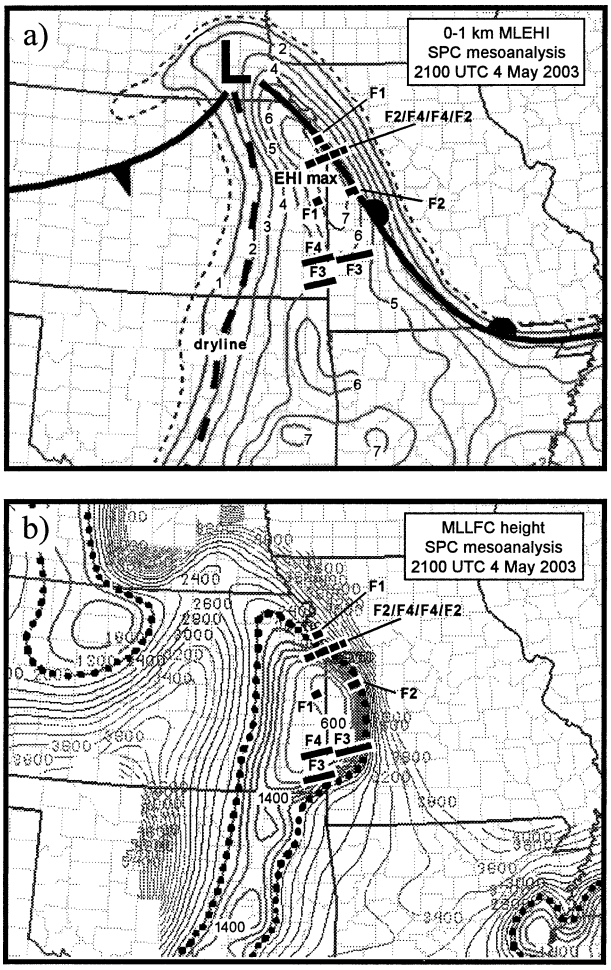

FIG. 10. Parameter fields of (a) 0–1-km MLEHI, and (b) approximated MLLFC height (in 200 m increments AGL) from RUC-based SPC mesoanalysis similar to Fig. 9, except at 2100 UTC 4 May 2003 over the Kansas–Missouri area. Surface features are shown in (a). Heavy dotted curves in (b) enclose areas of MLLFC height below 2000 m. Locations and F scales of tornadoes between 2100 and 2330 UTC are also shown in both (a) and (b).

9. LCL and LFC in large CIN environments

Recent research (RB98; Craven et al. 2002a; T03) has shown low LCL heights to be associated with tornadic storms, as noted in section 2. It should be emphasized that LCL height and LFC height are different thermodynamic variables; a low LFC implies a low LCL, but *the reverse is not true*. Figure 11 shows mean MLLCL and MLLFC heights for all supercells from the D03 database in this study by ascending ranges of MLCIN. It can be seen that LCL heights can remain relatively *low* as LFC heights become increasingly *high* and CIN larger. Furthermore, Fig. 12 shows 0–1-km shear and MLLCL for all tornado-warned cases in the D03 database with MLCIN $>$ 150 J kg^{-1} (58 cases). The area of the diagram enclosed by dashed lines corresponds to combinations of 0–1-km shear and MLLCL more likely to be associated with tornadoes from Craven et al. (2002a). Notice that none of the large CIN supercell cases from the D03 database that fell into this favorable parameter space produced F1 or greater intensity tornadoes. This shows that LCL height alone provides little direct information about whether instability in a particular environment is located above a layer of sizable CIN, which may have an impact on tornado potential.

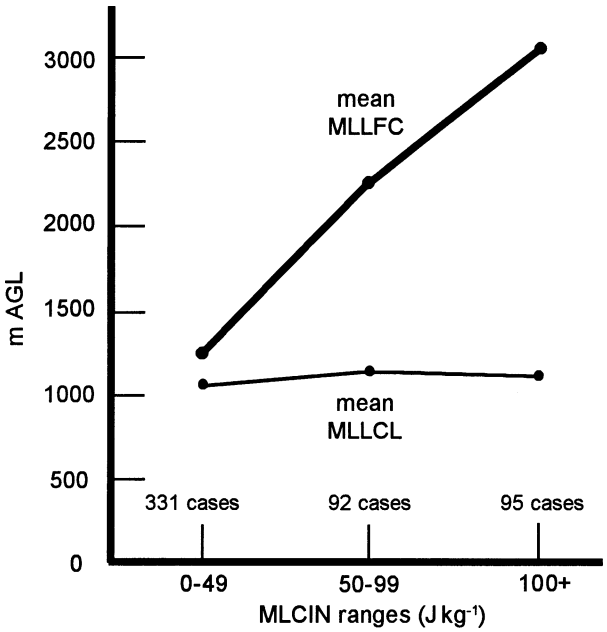

FIG. 11. Trends of mean MLLCL (thin line) and mean MLLFC (thick line) (m AGL) for all supercells in the D03 database by ascending ranges of MLCIN (J kg^{-1}). Number of cases in each range are also shown at bottom.

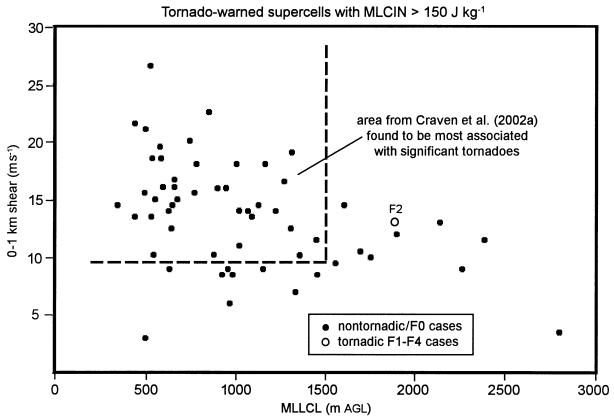

FIG. 12. The 0–1-km shear (m s^{-1}) and MLLCL (m AGL) for all tornado-warned supercell cases in the D03 database with MLCIN $>$ 150 J kg^{-1} (58 cases). Solid dots are nontornadic or F0 cases. Open circle is only tornado case of F1–F4 intensity. Area of diagram with 0–1-km shear $>$ 10 m s^{-1} and MLLCL $<$ 1500 m is enclosed by dashed lines.

10. Discussion and conclusions

Supercells in environments with mixed-layer and surface-based CAPE located above a layer of large CIN are not uncommon. In the D03 database used for this study, more than one-third of the supercell cases (187 of 518 cases) were associated with estimated MLCIN $\geq$ 50 J kg^{-1}, and nearly one-fifth (95 of 518 cases) occurred in environments with estimated MLCIN $\geq$ 100 J kg^{-1}. The relative number of supercells in these categories using SBCIN was similar but slightly larger.

Consistent with results regarding CIN in RB98, this study suggests that environments where CIN is large and LFC is high may impact the likelihood of tornadoes. In the D03 database, supercell tornadoes were most commonly associated with MLCIN less than 50 J kg^{-1} and MLLFC heights less than 2000 m. As MLCIN and MLLFC increased, frequency of F1–F4 tornadoes dropped considerably, to below 5% when MLCIN was larger than 150 J kg^{-1} and below 10% when MLLFC was higher than 3000 m. These results agree with a smaller database in a less formal study by Davies (2002). Using surface-based parcels, SBCIN and SBLFC yielded similar results, with a large percentage (75%) of F1–F4 tornado cases having SBCIN less than or roughly equal to MLCIN.

From a physical standpoint, an environment with large CIN and associated high LFC heights may inhibit low-level parcel ascent and stretching near the ground, reducing the likelihood of tornadoes. It is also possible that tornadogenesis may, in part, be related to rapid upward acceleration and stretching *within* the layer containing largest helicity. If CAPE is not positive and large within the same layer where SRH is large (e.g., CAPE located above and vertically ''disconnected'' from a layer of large SRH), then tornado development may become less likely. This latter idea is speculative, but is also a possible subject for future examination. Rasmussen (2003) introduced low-level CAPE (e.g., CAPE within the lowest 3 km AGL) as a parameter found to be associated with tornadic supercells in a reexamination of the database from RB98. This suggests that there may be a physical connection between low-level CAPE (associated with smaller CIN and lower LFC heights) and low-level SRH regarding tornado formation.

Table 4 shows the number of supercells in the D03 database that were specifically tornado warned, listed by ascending MLCIN range, along with the number of cases where F1–F4 intensity tornadoes were verified. Because the percentage of tornado-warned supercells producing F1–F4 tornadoes decreased with increasing MLCIN characteristics, the table suggests that tornado warning false alarms in some situations might be reduced if CIN or LFC were taken into account. A degree of restraint in issuing tornado warnings for supercells occurring in environments where MLCIN is larger than

TABLE 4. Summary of supercells from the D03 database associated with tornado warnings issued by NWS offices (477 cases), listed by MLCIN range. Number and percentage of F1–F4 intensity tornadoes verified are also listed, including number of cases with deaths.

MLCIN (J kg^{-1})	Tornado-warned supercells	F1–F4 tornadoes verified	% of tornado-warned supercells with F1–F4 tornadoes
0–49	306	132 (29 with deaths)	43%
50–99	81	22 (5 with deaths)	27%
100–149	32	8 (No deaths)	25%
$\geq$150	58	1 (No deaths)	2%

150–200 J kg^{-1} or MLLFC is higher than 3000–3500 m may result in some amount of reduction regarding tornado warning false alarms. Unless low-level and deep-layer shear are very large in such situations (section 7), severe thunderstorm warnings may be more appropriate.

Occasionally, supercell tornadoes do occur in environments where CIN is relatively large and LFC is relatively high. Corresponding cases in this study (section 7) suggested that these supercells tend to have larger amounts of 0–1-km SRH (e.g., 200–300 m^2 s^{-2} or more), resulting in large MLEHI values. Deep-layer shear also tended to be large (near 25 m s^{-1} or greater). However, the sample of tornado cases associated with MLCIN $\geq$ 100 J kg^{-1} in this study was too small to make conclusions, and more research is needed to clarify these results. The fact that only one tornado case of F1 or greater intensity occurred in the database with MLCIN greater than 150 J kg^{-1} does suggest that when low-level negative buoyancy is this large, the occurrence of significant (F2–F4) tornadoes is rare.

The importance of monitoring evolution of *observed* surface map features along with trends of model-derived fields to assess impact on MLCIN and MLLFC environments was seen in section 8, particularly with example 2. Even though a cool sector environment in a particular location may appear to have large CIN and high LFC characteristics, the near proximity of a front with notably smaller CIN and lower LFC heights to the south or west may be key. If a warm front is advancing and cool surface air is being replaced by air with smaller CIN, the environment near the front can change rapidly. These changes may not always be reflected properly by model-derived profiles. *Individual model-derived forecasts alone should not be relied on to diagnose relevant fields and nearby changes.* As noted in sections 6 and 7, it may also be important to monitor and compare surface-based computations; SBCIN may suggest noticably less negative buoyancy in low-levels than indicated by MLCIN.

In addition to cool sector environments having large CIN and high LFC heights, this study also highlighted warm sector settings that can have some of the same characteristics due to a warm mixed layer aloft. Example 3 in section 8 showed this type of environment, which is not uncommon in the plains of the United States when eastward advection of warm, dry air from the desert southwest takes place above a moist low-level layer. With surface cooling increasing CIN and LFC heights at night, this type of environment is probably one reason why nighttime and morning tornadoes are less common in the plains than in the Gulf coast states.

Section 9 showed that, compared to LFC, the height of the LCL is not directly useful in diagnosing environments with large low-level negative buoyancy. This makes sense because LCL is an estimate of cloud base, which can be low even when LFC is high and CIN is large. Recent research (RB98; Craven et al. 2002a; T03) has shown lower LCL heights to be associated with supercell tornadoes, but CIN and LFC also appear important because they relate to negative buoyancy in low levels that could reduce the likelihood of significant tornadoes based on empirical results in this study.

As seen in sections 5 and 6, the effect of the VTC on CIN and LFC height is not always negligible, and can impact the operational assessment of values. This suggests that forecasters be aware of whether the VTC is incorporated into operational software and products they use. For example, most RUC-based mesoanalysis products available from SPC (Bothwell et al. 2002) incorporate the VTC, while software products at many local NWS offices do not. Consistency regarding use of the VTC and thermodynamic computations in future software would seem to be desirable.

Finally, results from this study suggest many questions to be investigated in future field observation and modeling studies relating to supercells and tornadoes. For example, if it is largely rear-flank downdraft air that enters a developing tornado (Markowski et al. 2002), what relevance does CIN in the larger-scale storm environment have? Does increased CIN in the storm inflow environment actually reduce near-surface upward velocities? If so, to what degree can dynamic vertical pressure gradients overcome this? Does small CIN simply imply deeper moisture and large low-level relative humidity that can reduce near-surface cold pooling, or does it actually facilitate increased near-surface vertical velocities? How do storms modify CIN and LFC in their immediate environment? Although empirical evidence from this investigation suggests that near-storm CIN and LFC can impact tornadogenesis, these and other questions show that there is a great deal to learn about how low-level thermodynamic characteristics on a broad scale relate to tornadoes and processes in the local storm environment.

Acknowledgments. Rich Thompson and Roger Edwards (SPC), Bob Johns (SPC/CIMMS), and Matt Bunkers (NWS Rapid City, South Dakota) are gratefully acknowledged for providing helpful information and discussion at a preliminary stage of this project. Comments and suggestions by Barry Schwartz (FSL) and two anonymous reviewers were thought provoking and very helpful in clarifying focus, definitions, and terminology for this study. Finally, my father Boyd Davies helped give me the resources, patience, and resolve to complete this project.

REFERENCES

Baldwin, M. E., J. S. Kain, and M. P. Kay, 2002: Properties of the convection scheme in NCEP's Eta model that affect forecast sounding interpretation. *Wea. Forecasting,* **17,** 1063–1079.

Benjamin, S. G., J. M. Brown, K. J. Brundage, B. E. Schwartz, T. G. Smirnova, T. L. Smith, and L. L. Morone, 1998: RUC-2—The Rapid Update Cycle version 2. NWS Tech. Procedure Bull. No. 448, 18 pp.

——, and Coauthors, 2002: RUC20—The 20-km version of the Rapid Update Cycle. NWS Tech. Procedure Bull. No. 490, 29 pp.

——, and Coauthors, 2004: An hourly assimilation–forecast cycle: The RUC. *Mon. Wea. Rev.,* **132,** 495–518.

Bothwell, P. D., J. A. Hart, and R. L. Thompson, 2002: An integrated three-dimensional objective analysis scheme in use at the Storm Prediction Center. Preprints, *21st Conf. on Severe Local Storms,* San Antonio, TX, Amer. Meteor. Soc., J117–J120.

Colby, F. P., 1984: Convective inhibition as a predictor of convection during AVE-SESAME II. *Mon. Wea. Rev.,* **112,** 2239–2252.

Colman, B. R., 1990: Thunderstorms above frontal surfaces in environments without positive CAPE. Part I: A climatology. *Mon. Wea. Rev.,* **118,** 1103–1121.

Craven, J. P., H. E. Brooks, and J. A. Hart, 2002a: Baseline climatology of sounding derived parameters associated with deep, moist convection. Preprints, *21st Conf. on Severe Local Storms,* San Antonio, TX, Amer. Meteor. Soc., 643–646.

——, R. E. Jewell, and H. E. Brooks, 2002b: Comparison between observed convective cloud-base heights and lifting condensation level for two different lifting parcels. *Wea. Forecasting,* **17,** 885–890.

Davies, J. M., 1993: Hourly helicity, instability, and EHI in forecasting supercell tornadoes. Preprints, *17th Conf. on Severe Local Storms,* St. Louis, MO, Amer. Meteor. Soc., 107–111.

——, 2002: On low-level thermodynamic parameters associated with tornadic and nontornadic supercells. Preprints, *21st Conf. on Severe Local Storms,* San Antonio, TX, Amer. Meteor. Soc., 603–606.

Davies-Jones, R. P., D. Burgess, and M. Foster, 1990: Test of helicity as a tornado forecast parameter. Preprints, *16th Conf. on Severe Local Storms,* Kananaskis Park, AB, Canada, Amer. Meteor. Soc., 588–592.

Doswell, C. A., III, and E. N. Rasmussen, 1994: The effect of neglecting the virtual temperature correction on CAPE calculations. *Wea. Forecasting,* **9,** 625–629.

——, D. V. Baker, and C. A. Liles, 2002: Recognition of negative factors for severe weather potential: A case study. *Wea. Forecasting,* **17,** 937–954.

Hart, J. A., and W. Korotky, 1991: The SHARP workstation v1.50 user's guide. NOAA/National Weather Service, 30 pp. [Available from NWS Eastern Region Headquarters, 630 Johnson Ave., Bohemia, NY 11716.]

Lemon, L. R., 1977: New severe thunderstorm radar identification techniques and warning criteria: A preliminary report. NOAA Tech. Memo NWS NSSFC-1, 60 pp.

Maddox, R. A., L. R. Hoxit, and C. F. Chappell, 1980: A study of tornadic thunderstorm interactions with thermal boundaries. *Mon. Wea. Rev.,* **108,** 322–336.

Markowski, P. M., J. M. Straka, and E. N. Rasmussen, 2002: Direct surface thermodynamic observations within rear-flank downdrafts of nontornadic and tornadic supercells. *Mon. Wea. Rev.,* **130,** 1692–1721.

Moncrief, M., and M. J. Miller, 1976: The dynamics and simulation of tropical cumulonimbus and squall lines. *Quart. J. Roy. Meteor. Soc.,* **102,** 373–394.

Rasmussen, E. N., 2003: Refined supercell and tornado forecast parameters. *Wea. Forecasting,* **18,** 530–535.

——, and D. O. Blanchard, 1998: A baseline climatology of sounding-derived supercell and tornado forecast parameters. *Wea. Forecasting,* **13,** 1148–1164.

Rogers, E., T. L. Black, D. G. Deaven, G. J. DiMego, Q. Zhao, M. Baldwin, N. W. Junker, and Y. Lin, 1996: Changes to the operational ''early'' Eta analysis/forecast system at the National Centers for Environmental Prediction. *Wea. Forecasting,* **11,** 391–413.

Rotunno, R., and J. B. Klemp, 1982: The influence of the shear-induced pressure gradient on thunderstorm motion. *Mon. Wea. Rev.,* **110,** 136–151.

Thompson, R. L., R. Edwards, J. A. Hart, K. L. Elmore, and P. Markowski, 2003: Close proximity soundings within supercell environments obtained from the Rapid Update Cycle. *Wea. Forecasting,* **18,** 1243–1261.